Journal of Undergraduate Chemistry Research, **2026**, 25 (2), 54

EFFECT OF ALKANES ON THE FLUORESCENCE OF VAPOR DEPOSITED BIPHENYL ON Al_2O_3

Blake A. Bush*, Mirabelle M. Smith*, Vanessa H. Kragelund* and A.M. Nishimura†

Department of Chemistry, Westmont College, Santa Barbara, CA 93108

Abstract

Vacuum vapor deposition of biphenyl on a cold Al_2O_3 form amorphous adlayers that undergo disorder-to-order transition when the temperature of the adsorbent is ramped during the temperature programmed desorption (TPD) experiment. In bilayers where the underlayer is a simple alkane that desorbs at a lower temperature than the biphenyl overlayer, the fluorescence spectra can be used to determine the surface dynamics as voided space is formed when the underlayer desorbs. The structural reorganization due to the resulting thermally activated collapse of the suspended biphenyl layer is manifest in spectral and intensity changes.

†Corresponding author: nishimu@westmont.edu *Undergraduate researchers and co-authors

Keywords: adsorption, biphenyl, excimer, vapor deposition, desorption, temperature programmed desorption, TPD

Submitted: June 10, 2026 Accepted: July 3, 2026 Revision submitted: July 3, 2026 Published: July 4, 2027

Introduction

The fluorescence spectra of aromatic molecules are highly sensitive to the molecular environments created by surrounding solvent molecules.[1] If thin films of a fluorophore and a solvent are deposited as separate adlayers by physical vapor deposition, their interactions can be monitored through changes in fluorescence spectra and intensity.[2-12] During temperature-programmed desorption (TPD) experiments, in which the substrate temperature is linearly ramped, molecular dynamics occurring within the adsorbed films can be observed in real time through temperature-dependent fluorescence measurements.[2-12]

In a previous study, bilayers consisting of a fluorophore, naphthalene, and a simple *n*-alkane were prepared by vapor deposition onto Al_2O_3.[12] The *n*-alkanes were selected as underlayers because their desorption temperatures were lower than that of naphthalene. During TPD experiments, both the fluorescence spectra and emission intensities of the naphthalene overlayer were monitored.[12] As the alkane underlayer desorbed, it percolated through the naphthalene film and transiently solvated the fluorophore, producing characteristic monomer fluorescence. Following desorption of the underlayer, spectroscopic evidence suggested the presence of a voided space between the naphthalene overlayer and the Al_2O_3 substrate.[12] The discussion presented herein adopts and extends this voided space/suspended overlayer framework, which was not explicitly considered in the earlier work.

In the present study, biphenyl was used as the fluorophore. Unlike naphthalene, which is strictly planar, biphenyl possesses an additional conformational degree of freedom arising from rotation about the central C–C bond. Consequently, the fluorescence spectrum is sensitive to the biphenyl dihedral angle, allowing conformational changes to be monitored spectroscopically.[5,10] This property was exploited to investigate the formation of the voided space and the response of the biphenyl overlayer to the structural changes induced by underlayer desorption.

Upon vapor deposition onto Al_2O_3, biphenyl forms an amorphous adlayer. During TPD, several thermally activated processes occur that can influence the fluorescence spectra. As the substrate temperature approaches approximately 10 K below the desorption temperature of the *n*-alkane underlayer, alkane molecules begin to percolate through the biphenyl film, effectively solvating the fluorophore.[2-12] Subsequent desorption of the underlayer creates a voided region between the Al_2O_3 surface and the biphenyl overlayer. The suspended overlayer does not necessarily collapse immediately, but instead requires sufficient thermal energy to overcome the activation barrier associated with structural reorganization.

Simultaneously, biphenyl undergoes a disorder-to-order transition near 160 K when deposited directly on Al_2O_3, although the presence of an alkane underlayer may alter this transition temperature. In addition, biphenyl deposited on Al_2O_3 initially adopts a dihedral angle of approximately 45°, similar to that of the isolated gas-phase molecule.[5,6] As the temperature increases, the molecules may become more planar due to intermolecular dispersion interactions and enhanced packing efficiency during the disorder-to-order transition.[5,10] Consequently, the observed fluorescence spectra reflect the combined effects of underlayer percolation, void formation, overlayer collapse, conformational planarization, and structural ordering within the biphenyl film.

Experimental

Biphenyl and alkanes were of the highest purity (> 99%) were purchased from commercial sources (Sigma-Aldrich, St. Louis, MO; TCI, Portland, OR). They were placed in a sample holder attached to one end of a precision leak valve for vapor deposition. The ultra-high vacuum chamber had a background hydrogen base pressure of 1 x 10^{-9} Torr. A single crystal of Al_2O_3 (0001) (Crystal Systems, Inc., Salem, MA) was suspended on the lower end of a liquid nitrogen cryostat via copper post on either side of the Al_2O_3 with a sapphire spacer for both electrical and some degree of thermal isolation from the cryostat. Resistive heating of the Al_2O_3 was done by sending current through a thin tantalum foil that was in thermal contact with the substrate. A type-K (chromel/alumel) thermocouple (Omega, Norwalk, CT) that was also in thermal contact with the Al_2O_3 monitored the temperature. Process control during the TPD experiment was accomplished by a program written in LabVIEW (National Instruments, Austin, TX) that incorporated a PID (proportional-integral-derivative) feedback algorithm that linearly incremented the temperature of the Al_2O_3 crystal at 1.98 ± 0.01 K s^{-1} (roughly 2 K s^{-1}).

Optical pumping of the fluorophore was accomplished with a high pressure Hg lamp whose output was focussed through a 0.25 m monochrometer and λ_0 was set at 250 nm. Fluorescence emission from the adlayer on the Al_2O_3 was captured via a quartz lens and light pipe assembly was attached to the vacuum feed-

through that terminated at the spectrometer. During the TPD, the LabVIEW program took the fluorescence spectra every 300 ms in real time from an Ocean Optics SR2 UV-Vis spectrometer (Ocean Optics, Orlando, FL) that was sensitive in the ultra-violet. Manipulation of the array of spectra as a function of temperature by a MATLAB (Mathworks, Natick, MA) template yielded the wavelength-resolved TPD that are shown in the figures. To ensure a clean surface, the Al_2O_3 was heated to 300 K after each run. Temperature ramps to higher temperatures did not indicate any other adsorbates.[1-9]

Transmittance of the excitation light was detected with a photomultiplier whose output was sent to a computer interfaced high resolution analog-to-digital converter that the same LabVIEW program controlled. A UV shortpass optical filter had been placed in front of the photomultiplier (PMT) detector so that only the 250 nm excitation light was being monitored. The voltages from the photomultiplier at 0% and 100% transmittances were determined by blocking the excitation light and using the same optical configuration with a clean surface, respectively. In this way, the transmittance correlated linearly with the voltages from the photomultiplier. Sources of error are the fluctuation in the excitation light and PMT that gave low frequency and high frequency noise, respectively, and resulted in ± 3% error in the % transmittance.

Results

Upon heating, the vapor-deposited biphenyl film is expected to undergo several thermally activated structural relaxation processes. These include: (1) collapse of the voided volume created by desorption of the n-alkane underlayer; (2) structural reorganization and ordering of the biphenyl adlayer; and (3) the response of biphenyl to the evolving molecular environment during the disorder-to-order transition, including nucleation and growth of ordered domains.[12]

The temperature ranges over which void collapse and structural ordering occur may overlap, causing these processes to merge into a single observable event as the *n*-alkane underlayer is varied. Consequently, the fluorescence spectrum and intensity of biphenyl may reflect the combined effects of void collapse, molecular reorganization, conformational changes, and crystallization. Careful examination of the temperature-dependent spectral signatures is therefore necessary to distinguish the contributions of these competing processes and to understand their roles in determining the morphology of the biphenyl adlayer.

Multilayer biphenyl

Shown in Figure 1 is the wavelength-resolved temperature-programmed desorption (TPD) spectrum of multilayer biphenyl. In the gas phase, biphenyl adopts a twisted conformation with a dihedral angle of approximately 45°.[5,10] The fluorescence spectrum of the amorphous vapor-deposited adlayer exhibits a characteristic emission maximum at λ_{max} = 320 nm. As the temperature is increased during the TPD experiment, the fluorescence intensity gradually decreases due to thermal quenching.

At approximately 155 K, biphenyl begins to undergo a disorder-to-order transition that is completed by about 165 K. This transition is accompanied by a substantial decrease in fluorescence intensity, ultimately reaching approximately 10% of its initial value. The pronounced reduction in emission intensity is indicative of the high degree of structural ordering achieved in the crystalline phase. Concurrent with the disorder-to-order transition, the fluorescence spectrum undergoes a red shift from approximately 320 nm to 340 nm. Although subtle in the wavelength-resolved TPD plot, this spectral shift is consistent with increased intermolecular interactions and a more planar molecular conformation in the ordered biphenyl film.[1]

n-Pentane/biphenyl

Shown in Figure 2 is the wavelength-resolved TPD spectrum of biphenyl with an *n*-pentane underlayer. The fluorescence spectrum of the amorphous biphenyl adlayer initially exhibited an emission maximum at λ_{max} = 320 nm. Between approximately 130 and 135 K, the spectrum gradually red-shifted to λ_{max} = 340 nm. The disorder-to-order transition occurred at approximately 160 K; however, unlike multilayer biphenyl (Fig. 1), the emission maximum remained at 340 nm throughout the transition.

Shown in Figure 3 are representative transmittance plots as a function of temperature for biphenyl deposited on an *n*-pentane underlayer. Control experiments consisted of *n*-pentane alone ($\Theta_{biphenyl}$ = 0, indicated by *) and biphenyl alone ($\Theta_{n\text{-}pentane}$ = 0, indicated by 0). With the exception of a pronounced decrease in transmittance during *n*-pentane percolation and desorption, the transmittance remained relatively constant throughout the TPD experiment. Furthermore, transmittance decreased systematically with increasing *n*-pentane coverage despite a constant biphenyl coverage.

One possible explanation for the enhanced fluorescence in-

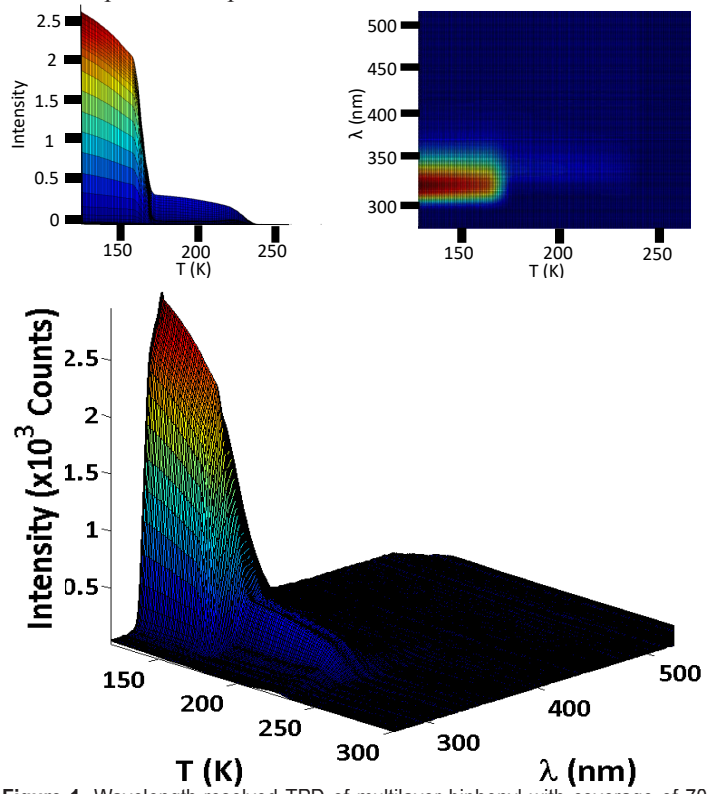

Figure 1. Wavelength-resolved TPD of multilayer biphenyl with coverage of 70 ML. The amorphous biphenyl fluorescence has λ_{max} = 320 nm. The disorder-to-order transition occurs at 160 K and red-shifts to 340 nm with a concommitant decrease in the intensity to about 10%, and is barely visible. Left inset: Intensity vs. T during the TPD. Right inset: top view.

tensity is increased absorption of the excitation light by the biphenyl adlayer. Such behavior could arise if percolation of *n*-pentane through the film produced greater spatial separation between biphenyl molecules, thereby reducing aggregation-induced quenching and increasing the fluorescence quantum yield. A second notable observation is that the characteristic transmittance step associated with the disorder-to-order transition of multilayer biphenyl at approximately 160 K was absent when *n*-pentane was present as the underlayer. This suggests that the conventional disorder-to-order transition was substantially altered by the presence of the underlayer.

As shown in Figure 3, *n*-pentane alone scattered approximately 12% of the excitation light at a coverage of ~136 ML, while a 100 ML biphenyl film absorbed approximately 15%. Consequently, the measured transmittance of the bilayer at a biphenyl coverage of 114 ML is reasonably consistent with the combined optical effects expected from the two individual films. The sharp decrease in transmittance near 130 K coincides with *n*-pentane percolation and desorption. Although transient scattering undoubtedly contributes to this decrease, the magnitude of the effect appears too large to be explained by scattering alone. An additional contribution may arise from transient solvation of biphenyl by *n*-pentane during percolation through the adlayer. Another possibility that cannot be excluded is that collapse of the voided space requires very little activation energy and therefore occurs nearly simultaneously with underlayer desorption.

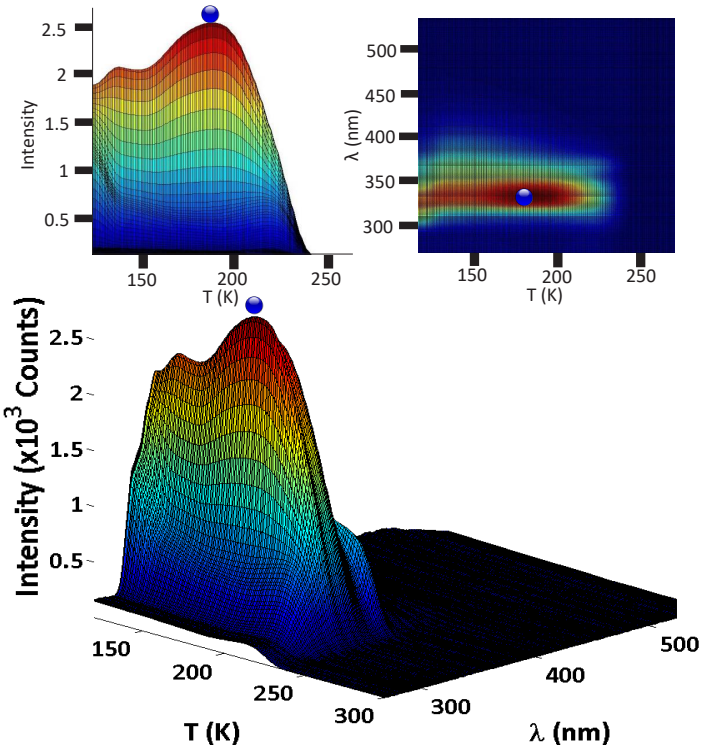

Figure 2. Wavelength-resolved TPD of biphenyl with coverage of 110 ML with an underlayer of n-pentane at a coverage of 110 ML. The amorphous biphenyl begins with λ_{max} = 320 nm. From 130 K, red-shift occurs with λ_{max} = 340 nm at 135 K. The disorder-to-order transition occurs at 160 K and red-shifts to 340 nm. The maximum fluorescence emission from defects occurred at 190 K. Blue ball indicates the maximum fluorescence that was plotted in Fig. 4.Left inset: Intensity vs. T during the TPD. Right inset: top view.

Because λ_{max} remained fixed at 340 nm throughout the remainder of the TPD experiment, the biphenyl adlayer did not exhibit the spectral signature characteristic of the usual disorder-to-order transition. One interpretation is that the film remained substantially disordered following reorganization. Alternatively, the reorganized film may have become ordered while retaining a sufficiently high density of defects to produce a morphology that is very fluorescent. Additional transmittance data supporting these observations are presented in Figures S2–S5.

Shown in Figure 4 is a plot of the normalized maximum fluorescence intensity at 340 nm measured at 190 K as a function of the coverage ratio $\Theta_{n\text{-pentane}}(ML)/\Theta_{biphenyl}(ML)$. To compensate for small variations in biphenyl deposition, the maximum fluorescence intensities were normalized to their respective initial intensities. A distinct change in slope occurs at approximately $\Theta_{n\text{-pentane}}/\Theta_{biphenyl} \approx 0.8$.

The fluorescence maximum at 190 K is tentatively attributed to collapse of the voided space followed by structural reorganization of the biphenyl adlayer. Such reorganization may increase the density of defects, including grain boundaries formed where microcrystalline domains meet.[13,14] At temperatures approximately 30 K below the desorption temperature of biphenyl, the adlayer may be regarded as a relatively mobile, plastic-like phase in which surface diffusion, molecular reorientation, nucleation, and crystallization are facilitated. Since *n*-pentane desorbs at approximately 132 K and the fluorescence maximum occurs near 190 K, the corresponding activation interval for this reorganization process is approximately 58 K.

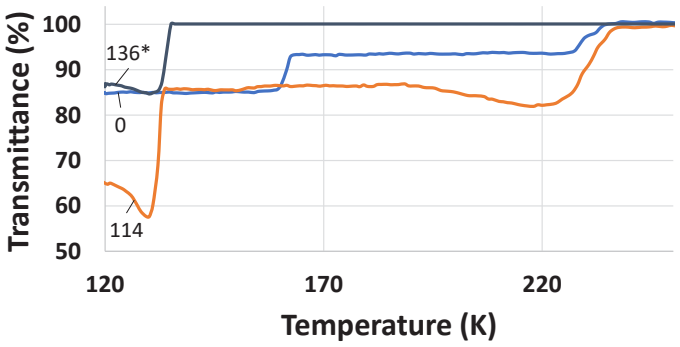

Figure 3. Plot of the transmittance of bilayer of n-pentane and biphenyl with $\Theta_{n\text{-pentane}}$ = 114 ML with $\Theta_{biphenyl}$ = 98 ML that had been deposited at 117 K with n-pentane as underlayer. 0⇨$\Theta_{n\text{-pentane}}$ =0, $\Theta_{biphenyl}$ = 70 ML ; *⇨$\Theta_{biphenyl}$ = 0, $\Theta_{n\text{-pentane}}$ = 136 ML.

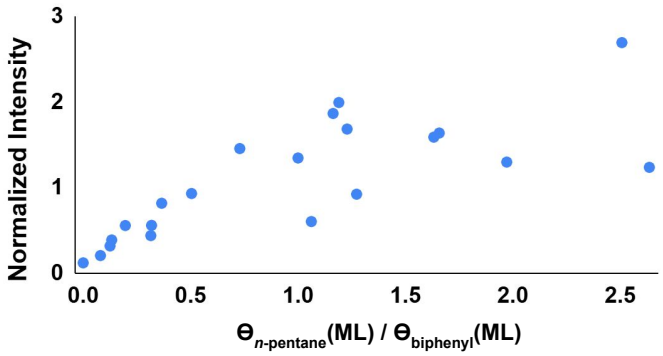

Figure 4. Plot of the normalized fluorescence intensity of the trap at 340 nm at 190 K relative to the intensity at the onset of TPD. as a function of $\Theta_{n\text{-pentane}}/\Theta_{bipehenyl}$. $\Theta_{naphthalenel}$ = 110 ±11 ML The inflection occurs at 0.8 $\Theta_{n\text{-pentane}}/\Theta_{biphenyl.}$

n-Hexane/biphenyl

Shown in Figure 5 is the wavelength-resolved TPD spectrum of biphenyl with an *n*-hexane underlayer. The peak desorption temperature of *n*-hexane was approximately 150 K, only about 10 K lower than the disorder-to-order transition temperature of biphenyl.

Presented in Figure 6 are the corresponding transmittance plots. These traces are qualitatively similar to those observed for the *n*-pentane/biphenyl bilayer. As before, the pronounced decrease in transmittance observed during *n*-hexane desorption is tentatively attributed to transient solvation of biphenyl by *n*-hexane as the latter percolates through the overlayer. In addition, the transmittance levels off at approximately the same value observed for multilayer biphenyl prior to its disorder-to-order transition. This observation suggests that the biphenyl adlayer retains a degree of disorder comparable to that of the amorphous multilayer, even after the temperature exceeds the normal disorder-to-order transition temperature of approximately 160 K.

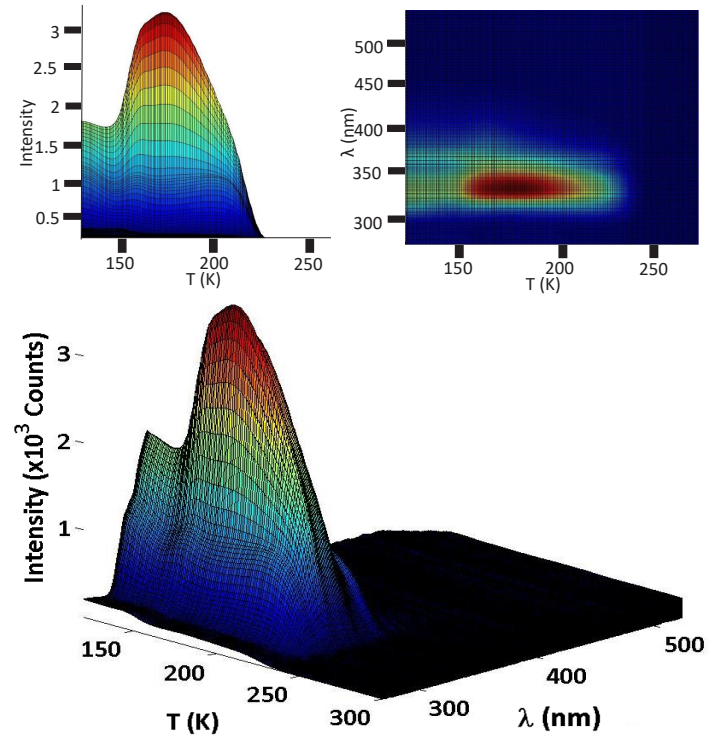

Figure 5. Wavelength-resolved TPD of biphenyl with coverage of 136 ML with an underlayer of n-hexane at a coverage of 110 ML. The amorphous biphenyl begins with λ_{max} = 340 nm. The disorder-to-order transition occurs at 160 K and continues at 340 nm a maximum trap intensity at 173 K. Left inset: Intensity vs. T during the TPD. Right inset: top view.

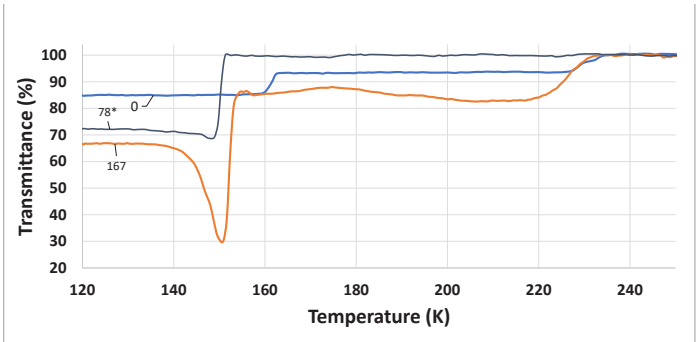

Figure 6. Plot of the transmittance of bilayer of n-hexane with $\Theta_{n\text{-hexne}}$ = 167 ML with $\Theta_{biphenyl}$ = 103 ML that had been deposited at 117 K with an with n-hexane as underlayer. 0⇨$\Theta_{n\text{-hexane}}$ =0, $\Theta_{biphenyl}$ = 70 ML ; *⇨$\Theta_{biphenyl}$ = 0, $\Theta_{n\text{-hexane}}$ = 78 ML.

Shown in Figure 7 is a plot of the normalized maximum fluorescence intensity at 173 K as a function of the coverage ratio $\Theta_{n\text{-hexane}}(ML)/\Theta_{biphenyl}(ML)$. To account for small variations in biphenyl deposition, the maximum fluorescence intensities were normalized to their respective initial values. A distinct change in slope is observed at approximately $\Theta_{n\text{-hexane}}/\Theta_{biphenyl} \approx 0.1$, indicating that only a relatively small amount of *n*-hexane is required to produce the maximum fluorescence response.

This unusually low coverage ratio is consistent with the close proximity of the *n*-hexane desorption temperature to the intrinsic disorder-to-order transition temperature of biphenyl. As discussed above, when void collapse and structural ordering occur over similar temperature ranges, the two processes may become coupled and appear as a single observable event. Under these conditions, the efficiency with which the underlayer modifies the biphenyl morphology is enhanced, allowing relatively small amounts of *n*-hexane to produce substantial changes in fluorescence intensity.

The maximum fluorescence intensity occurs at approximately 173 K, whereas the peak desorption temperature of *n*-hexane is approximately 150 K. Within the framework of the voided space/suspended overlayer model, the difference of approximately 23 K is interpreted as the activation interval required for collapse and reorganization of the suspended biphenyl overlayer following desorption of the *n*-hexane underlayer.

n-Heptane/biphenyl

Shown in Figure 8 is the wavelength-resolved TPD spectrum of a bilayer consisting of 102 ML of *n*-heptane and a 112 ML biphenyl overlayer. Notably, the peak desorption temperature of *n*-heptane was approximately 161 K, nearly coincident with the intrinsic disorder-to-order transition temperature of biphenyl. The maximum fluorescence intensity was observed at approximately 190 K. Within the framework of the voided space/suspended overlayer model, the difference of approximately 29 K is interpreted as the activation interval associated with collapse and reorganization of the biphenyl overlayer following desorption of the *n*-heptane underlayer.

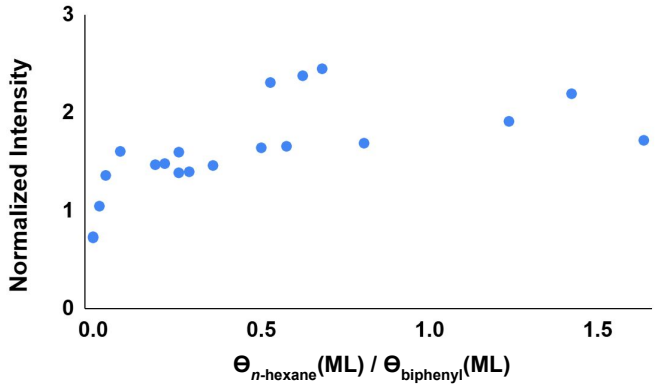

Figure 7. Plot of the normalized fluorescence intensity of the trap at 340 nm at 173 K relative to the intensity at the onset of TPD. as a function of $\Theta_{n\text{-hexane}}/\Theta_{bipehenyl}$. $\Theta_{biphenyl}$ = 120 ±19 ML Change in slopes was at 0.1 $\Theta_{n\text{-hexane}}/\Theta_{biphenyl}$.

The corresponding transmittance measurements (Cf. Figure 9) again exhibited a pronounced decrease near the *n*-heptane desorption temperature. As discussed for *n*-pentane and *n*-hexane, this behavior is tentatively attributed to a combination of transient scattering and solvation of biphenyl by *n*-heptane as it percolates through the overlayer. Following desorption of the underlayer, the transmittance returned to a value similar to that observed for amorphous biphenyl prior to its disorder-to-order transition. This observation suggests that the biphenyl adlayer retained a significant degree of disorder, even after the temperature exceeded the nominal transition temperature.

Shown in Figure 10 is a plot of the normalized maximum fluorescence intensity as a function of the coverage ratio $\Theta_{n\text{-heptane}}(ML)/\Theta_{biphenyl}(ML)$. The fluorescence response reaches saturation at substantially higher coverage ratios than observed for *n*-pentane or *n*-hexane. One possible explanation is that *n*-heptane possesses a greater probability of adopting one or more gauche conformations because of its increased conformational freedom.[15] Consequently, the molecule would have a smaller effective projection normal to the Al_2O_3 surface and may be less effective at perturbing the biphenyl overlayer during percolation and desorption. Within this interpretation, a larger number of *n*-heptane molecules is required to produce the same degree of structural disruption, thereby shifting the saturation point to higher coverage ratios.

n-Octane/biphenyl

Shown in Figure 11 is the wavelength-resolved TPD spectrum of biphenyl with an *n*-octane underlayer. The peak desorption temperature of *n*-octane was approximately 178 K, substantially higher than the intrinsic disorder-to-order transition temperature of biphenyl. The data shown correspond to a relatively low *n*-octane coverage, for which the fluorescence initially exhibited excimer emission with λ_{max} = 370 nm. As the temperature increased, the spectrum transitioned to trap emission at approximately 168 K, about 8 K higher than the disorder-to-order transition temperature observed for multilayer biphenyl.

The maximum fluorescence intensity was observed at approximately 195 K, corresponding to an activation interval of about 17 K relative to the *n*-octane desorption temperature. It should also be noted that the temperature of maximum fluorescence increased with increasing *n*-octane coverage, shifting from approximately 190 K at 55 ML to nearly 200 K for coverages greater than 100 ML. This behavior suggests that the extent of structural reorganization depends on the amount of *n*-octane present in the underlayer.

Shown in Figure 12 are the corresponding transmittance plots. In contrast to the other *n*-alkanes, the transmittance remained comparatively low over a broad temperature range, indicating substantial absorption of the excitation light by the biphenyl adlayer. This enhanced absorption is consistent with the unusually intense fluorescence relative to the initial intensity observed for the *n*-octane/biphenyl bilaye, similar to the data displayed in Figure 14.

Figure 13 presents the normalized maximum trap intensity as a function of the coverage ratio $\Theta_{n\text{-octane}}(ML)/\Theta_{biphenyl}(ML)$. As noted in the figure caption, the scatter in the data was sufficiently large that a reliable change in slope could not be determined. Consequently, unlike *n*-pentane, *n*-hexane, and *n*-heptane, the trap intensity does not exhibit a clear correlation with *n*-octane coverage.

One possible explanation is that trap formation depends not only on the extent of structural perturbation induced by the underlayer, but also on the stochastic processes of nucleation and crystallization. Because nucleation events occur randomly, the resulting density of crystalline defects, including grain boundaries formed between ordered domains, may vary significantly from experiment to experiment.[13,14] Consequently, the maximum trap fluorescence intensity of the ordered biphenyl adlayer may be governed primarily by the density and distribution of these defect sites rather than directly by the amount of *n*-octane present in the underlayer.[13]

Discussion

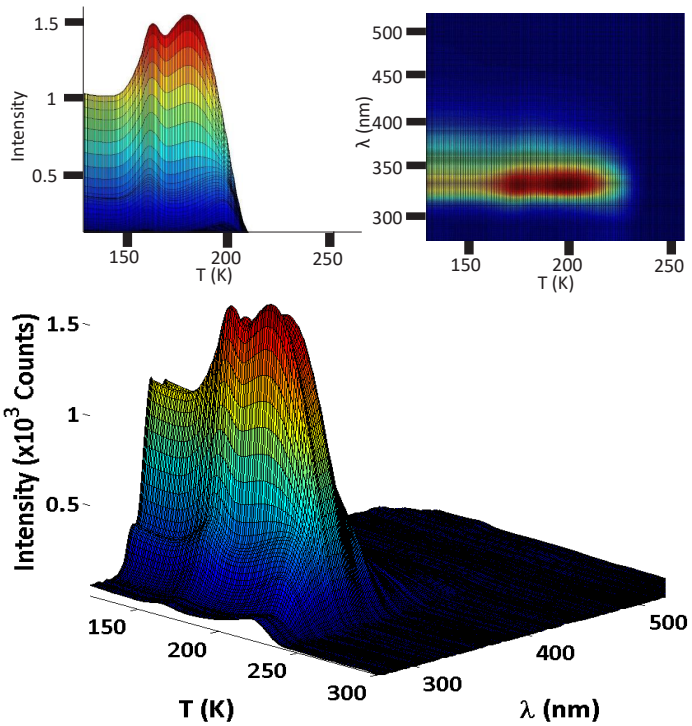

Figure 8. Wavelength-resolved TPD of biphenyl with coverage of 112 ML with an underlayer of n-heptane at a coverage of 102 ML. The amorphous biphenyl begins with λ_{max} = 340 nm and is constant through the TPD. The disorder-to-order transition occurs at 160 K. The maximum fluorescence emission from defects occurred at 190 K. Left inset: Intensity vs. T during the TPD. Right inset: top view.

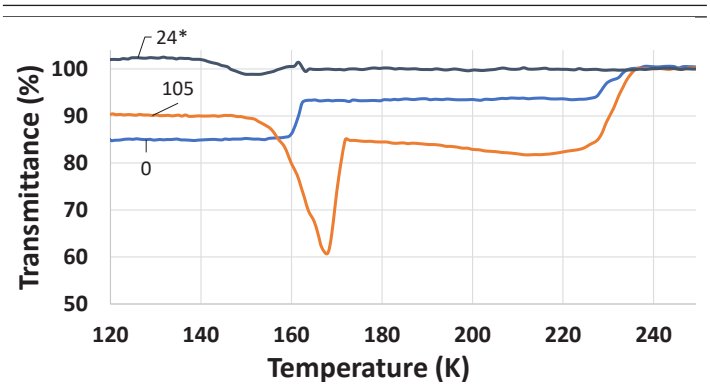

Figure 9. Plot of the transmittance of bilayer of n-heptane as a function of $\Theta_{n\text{-heptane}}$ = 105 ML with $\Theta_{biphenyll}$ = 112 ML that had been deposited at 117 K with n-heptane as underlayer. 0⇨$\Theta_{n\text{-heptane}}$=0, $\Theta_{biphenyl}$ = 70 ML ; *⇨$\Theta_{biphenyl}$ = 0, $\Theta_{n\text{-heptane}}$=24 ML

The summary plot shown in Figure 14 compares the initial and maximum trap fluorescence intensities for the four *n*-alkane underlayers. Several observations emerge from these data. For *n*-pentane, molecular aggregation is evidenced by the observation of the twisted biphenyl conformer characteristic of multilayer biphenyl. This suggests that, at lower *n*-pentane coverages, aggregation produces a heterogeneous landscape of molecular islands separated by exposed regions of the Al_2O_3 surface, allowing a fraction of the biphenyl molecules to adsorb directly on the substrate as in multilayer biphenyl (Cf. Fig. 1). As *n*-pentane desorbs and percolates through the biphenyl adlayer, the biphenyl becomes solvated and adopts a more planar conformation that is retained throughout the remainder of the TPD experiment. Similar behavior is observed for *n*-hexane, where dispersion forces are believed to promote aggregation and preferential orientation of the alkane clusters normal to the surface.[16,17]

The initial fluorescence intensities shown in Figure 14 are consistent with a distance-dependent interaction between biphenyl and the Al_2O_3 surface.[18] The increase in initial intensity from *n*-pentane to *n*-hexane suggests that these alkanes elevate the biphenyl layer farther from the substrate, thereby reducing surface-induced quenching. The subsequent decrease observed for *n*-heptane and *n*-octane is consistent with increased conformational freedom in

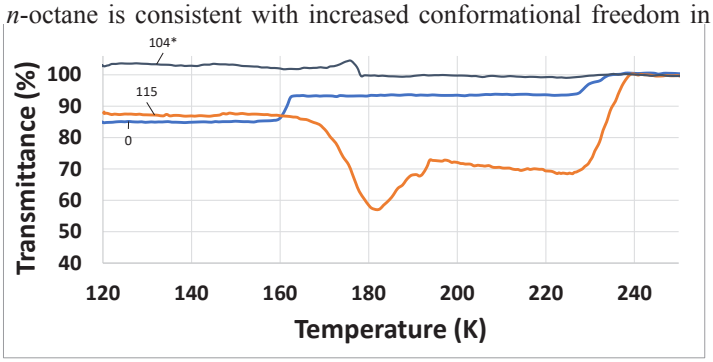

Figure 12. Plot of the transmittance of bilayer of n-octane $\Theta_{n\text{-octane}}$ = 115 ML with $\Theta_{biphenyl}$ = 104 ML that had been deposited at 117 K with n-octane as underlayer. 0⇨$\Theta_{n\text{-octane}}$=0, $\Theta_{biphenyl}$ = 70 ML ; *⇨$\Theta_{biphenyl}$ = 0, $\Theta_{n\text{-octane}}$ = 104 ML

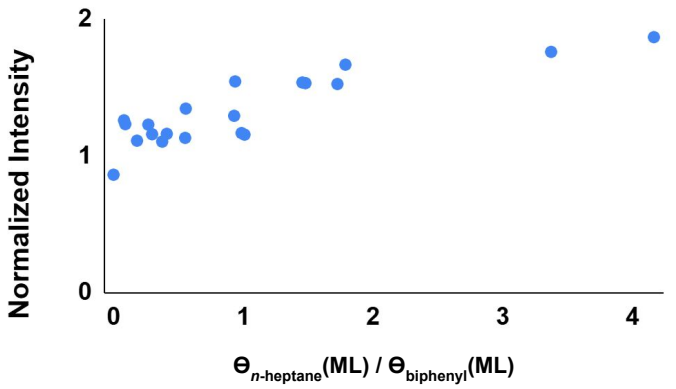

Figure 10. Plot of the normalized fluorescence intensity of the trap at 340 nm at 190 K relative to the intensity at the onset of TPD. as a function of $\Theta_{n\text{-heptane}}/\Theta_{bipehenyl}$. $\Theta_{biphenyl}$ = 110 ± 21 ML Change in slopes was at ~ 3 $\Theta_{n\text{-heptane}}/\Theta_{biphenyl}$.

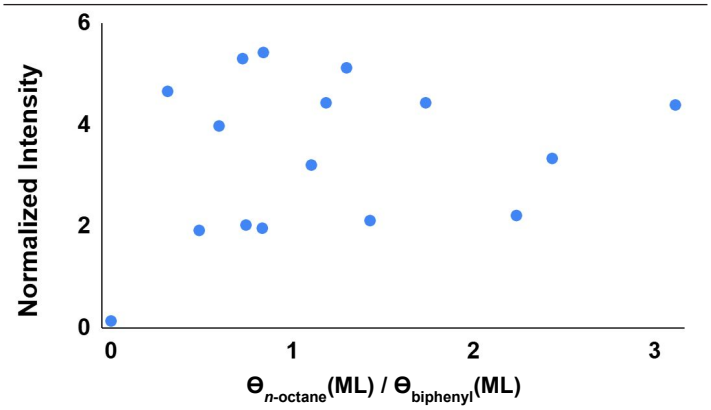

Figure 13. Plot of the normalized fluorescence intensity of the trap at 340 nm at 190 K relative to the intensity at the onset of TPD. as a function of $\Theta_{n\text{-octane}}/\Theta_{bipehenyl}$. $\Theta_{biphenyl}$ = 100 ±19 ML Scatter in the data makes it impossible to determine any slopes.

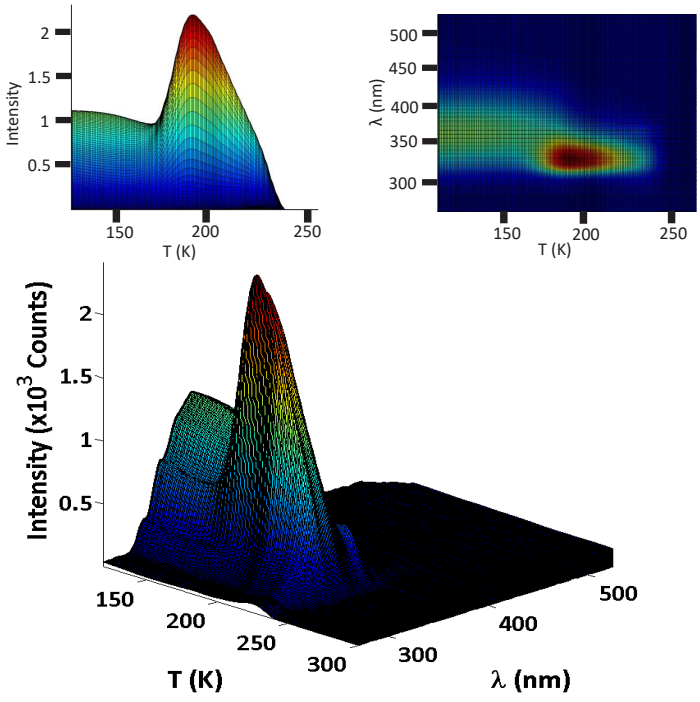

Figure 11. Wavelength-resolved TPD of biphenyl with coverage of 113 ML with an underlayer of n-octane at a coverage of 55 ML. The amorphous biphenyl begins with λ_{max} = 370 nm and forms excimers. The disorder-to-order transition occurs at 160 K where the excimer becomes traps. The maximum fluorescence emission from defects occurred at 190 K. Left inset: Intensity vs. T during the TPD. Right inset: top view.

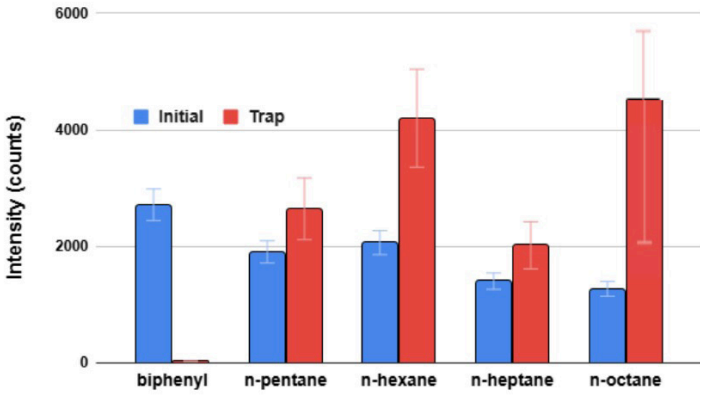

Figure 14. Summary of the averaged intensities of biphenyl with the n-alkane underlayers for the initial and trap intensities. The initial intensities depend on proximity of the biphenyl to the surface of Al_2O_3; the initial intensities increase from pentane to hexane because they are normal to the surface, but decrease with heptane and octane because of gauche conformers. The trap intensities follow the same trend except with octane, the disorder-to-order transition has caused the adlayer to order; the collapse occurs, and occurs very close to the desorption temperature: the higher the temperature, the easier the crystallization and the density of defect sites consequently increase.

the longer-chain alkanes. In this interpretation, one or more C–C bonds may adopt gauche conformations, reducing the effective molecular dimension normal to the surface.[15]

The trap intensities generally follow the same trend. An exception is *n*-octane, for which the disorder-to-order transition of biphenyl largely precedes underlayer desorption. Consequently, collapse of the voided space occurs at temperatures much closer to the desorption temperature of biphenyl, where molecular mobility, nucleation, and crystallization are more facile. The resulting increase in defect formation provides a plausible explanation for the unusually relative intense trap fluorescence observed for *n*-octane.

The morphologies created by *n*-heptane and *n*-octane appear to be substantially more disordered than those produced by *n*-pentane and *n*-hexane. Evidence for this is provided by the immediate formation of biphenyl excimer emission following deposition onto these surfaces. For *n*-heptane, excimer fluorescence dominates at coverages below approximately 50 ML (cf. Fig. S1), whereas at higher coverages, such as those shown in Figure 8, the planar conformer is initially observed. A similar trend is observed for *n*-octane. Because excimer formation in biphenyl requires an amorphous environment,[1,9] the low-coverage heptane and octane surfaces must be sufficiently rough and disordered to promote excimer formation. One possible source of this disorder is the increased probability of gauche conformations in the longer-chain alkanes, which would hinder efficient packing and reduce the tendency to form ordered molecular arrays. At higher coverages, however, the larger number of molecules may smooth the overall surface morphology and promote formation of the planar conformer.

The *n*-octane system appears to be distinguished by a highly stochastic nucleation and crystallization process.[13] This interpretation is supported by the absence of a clear correlation between trap intensity and *n*-octane coverage (cf. Fig. 13). Based on the trend established by the other alkanes in Figure 14, a lower trap intensity would have been expected for *n*-octane. Instead, the observed relative fluorescence intensity is substantially higher than anticipated. This behavior suggests that while nucleation may occur randomly, once initiated it can trigger crystallization pathways that generate a high density of fluorescent defect sites.

Although the effects observed here are less pronounced than those reported previously for naphthalene overlayers,[10] incorporation of the voided space/suspended overlayer model provides a more comprehensive framework for interpreting the behavior of biphenyl deposited on simple alkane underlayers. The combined fluorescence, transmittance, and coverage-dependent measurements are consistent with a picture in which underlayer desorption creates a transient voided region whose collapse, coupled with structural reorganization of the biphenyl film, governs the observed spectroscopic response.

Acknowledgment

The authors would like to thank the John Stauffer Charitable Trust for funding the student stipends for summer research. This work was supported by the donors of ACS Petroleum Research Fund under Undergraduate Research #68385-UR5 .

References

1. J.B. Birks. *Photophysics of Aromatic Molecules*, John Wiley & Sons Ltd., New York, NY (1970), pp. 301-370.
2. J.M. Rosenfeld, R.M. Toepfer, A.O. Lopez, J.C. Nieman, I. Felix, J. Zerwas and A.M. Nishimura, *JUCR*, **2024.** 23, 25-30.
3. I.Z. Song, S.T. Watanabe and A.M. Nishimura, *JUCR*, **2023**, 22, 78-85.
4. A.O. Lopez, B.X. Moses, C.D. Tobey, J. Arrieta, M. Ticas, J. Zerwas amd A.M. Nishimura, *JUCR*, **2025**, 24, 59-65.
5. M.K. Condie, Z.E. Moreau and A.M. Nishimura *JUCR*, **2019**, 18, 15-18.
6. M.K. Condie, B.D. Fonda, Z.E. Moreau and A.M. Nishimura, *Thin Solid Films*, **2020**, 697, 137823-137828.
7. B.D. Fonda, Z.I. Shih, J.J. Wong, L.G. Foltz, K.A. Martin and A.M. Nishimura, *JUCR*, **2018**, 17, 32-35.
8. K.L. Nili, Z.E. Moreau and A.M. Nishimura, *JUCR*, **2020**, 19, 19-23.
9. M.K. Condie, C. Kim, Z.E. Moreau, B. Dionisio, K. Nili, J. Francis, C. Tran, S. Nakaoka and A.M. Nishimura, *JUCR*, **2020**, 19, 14-17.
10. N.M. Bond and A.M. Nishimura, *JUCR*, **2022**, 21, 84-92.
11. A.O. Lopez, J.C. Nieman, J.M. Rosenfeld, R.M. Toepfer and A.M. Nishimura, *JUCR*, **2024**, 23, 16-23.
12. V. Kragelund, B. Bush, M. Smith and A.M. Nishimura, JUCR, 2026, submitted.
13. K. Kojima, *Prog. Crystal Growth and Charact.* **1991**, 23, 369-420
14. R.S. Smith, C. Huang, E.K.L. Wong, B.D. Kay, *Surf. Sci*., **1996,** L13-L18.
15. T. Tynkkynen, T. Hassien, M. Tiainen, P. Soininen, R. Laatikainen, Magnetic Resonance In Chemistry, **2012**, 50, 598-607.
16. C.M. Aubuchon, B.S. Davison, A.M. Nishimura and N.J. Tro, *J. Phys Chem.* **1994**, 98, 240-244.
17. R.M. Slayton, C.M. Aubuchon, T.L. Camis, A.R. Noble and N.J. Tro. *J. Phys. Chem*., **1995**, 99, 2151-2154.
18. D.R. Haynes, K.R. Helwig, N.J. Tro and S.M. George, *J. Chem. Phys.* **1990**, 93, 2836-2847.

Supplemental Materials

Low coverage n-heptane/biphenyl: S1

With low *n*-heptane coverage, less than 50 ML, the fluorescence from biphenyl is completely excimeric.

Transmittance of n-alkanes/biphenyl: S2-S5

Plots of transmittance at various coverges for *n*-alkane/biphenyl bilayers.

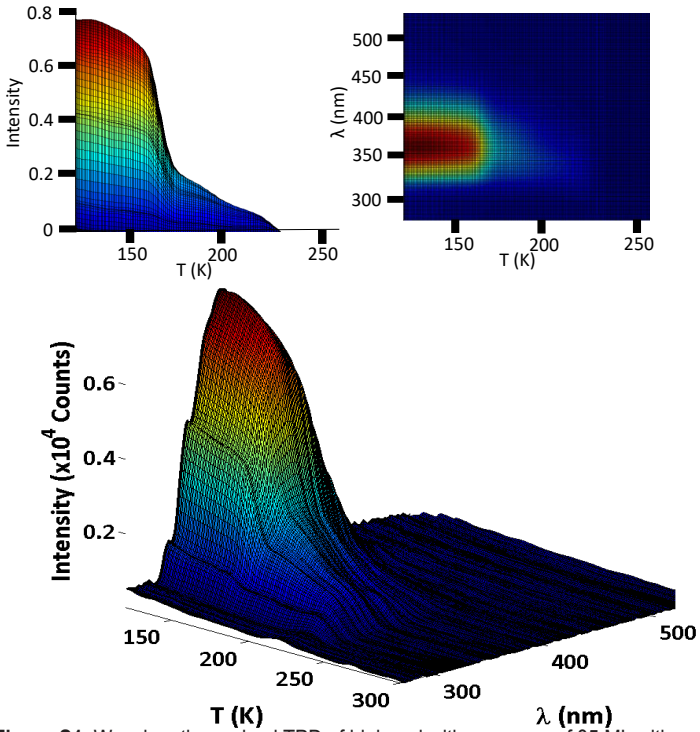

Figure S1. Wavelength-resolved TPD of biphenyl with coverage of 85 ML with an underlayer of n-heptane at a coverage of 13 ML. The amorphous biphenyl begins with λ_{max} = 370 nm initially and is the excimer. The disorder-to-order transition occurs at 160 K blue shifts to λ_{max} = 340 nm. Left inset: Intensity vs. T during the TPD. Right inset: top view.

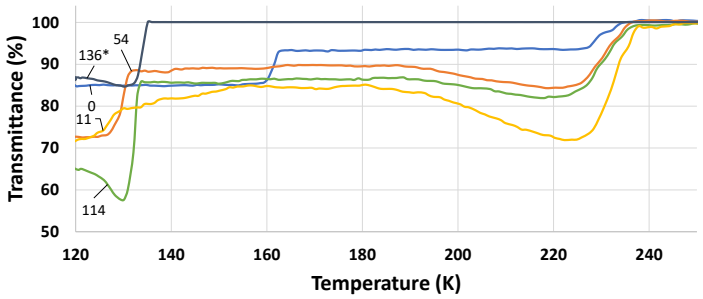

Figure S2. Plot of the transmittance of bilayer with varying n-pentane as a function of $\Theta_{n\text{-pentane}}$ with $\Theta_{biphenyl}$ = 102 ± 25 ML that had been deposited at 117 K with an underlayer of n-pentane. 0⇨$\Theta_{n\text{-pentane}}$ =0, $\Theta_{biphenyl}$ = 70 ML ; *⇨$\Theta_{biphenyl}$ = 0, only underlayer at the indicated coverage.

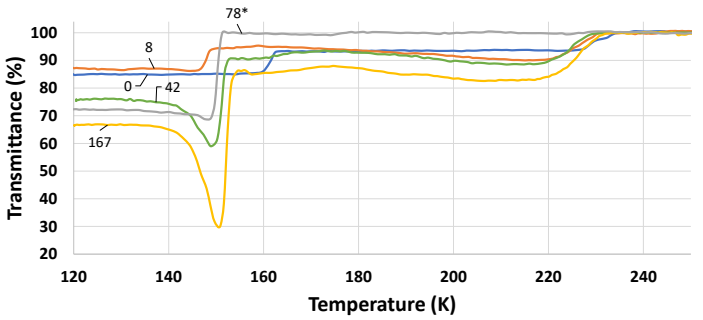

Figure S3. Plot of the transmittance of bilayer with varying n-hexane as a function of $\Theta_{n\text{-hexne}}$ with $\Theta_{biphenyl}$ = 115 ± 32 ML that had been deposited at 117 K with an with an underlayer of n-hexane. 0⇨$\Theta_{n\text{-hexane}}$ =0, $\Theta_{biphenyl}$ = 70 ML ; *⇨$\Theta_{biphenyl}$ = 0, only underlayer.

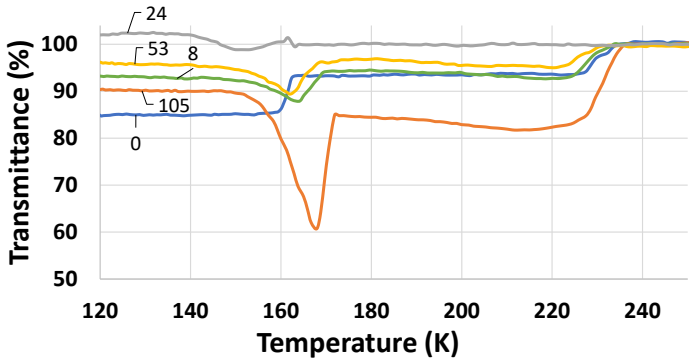

Figure S4. Plot of the transmittance of bilayer with varying n-heptane as a function of $\Theta_{n\text{-heptane}}$ with $\Theta_{biphenyll}$ = 107 ± 21 ML that had been deposited at 117 K with an underlayer of n-heptane. 0⇨$\Theta_{n\text{-heptane}}$ =0, $\Theta_{biphenyl}$ = 70 ML ; *⇨$\Theta_{biphenyl}$ = 0, only underlayer.

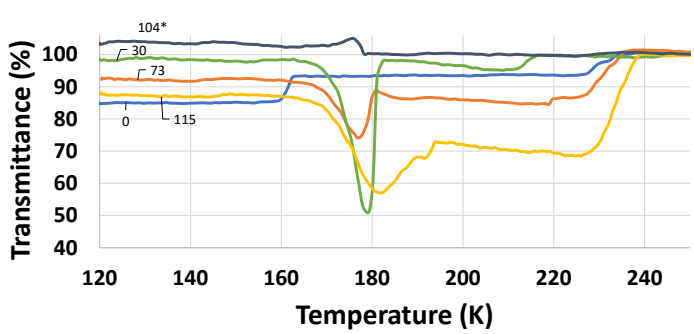

Figure S5. Plot of the transmittance of bilayer with varying n-octane as a function of $\Theta_{n\text{-octane}}$ with $\Theta_{biphenyl}$ = 103 ± 19 ML that had been deposited at 117 K with an underlayer of n-octane. 0⇨$\Theta_{n\text{-octane}}$ =0, $\Theta_{biphenyl}$ = 70 ML ; *⇨$\Theta_{biphenyl}$ = 0, only underlayer.